HIGH-RESOLUTION URBAN AREA MAP FOR 3372 CITIES OF THE WORLD

Hiroyuki Miyazaki[1], Koichiro Itabashi[2], Xiaowei Shao[1], Koki Iwao[3], and Ryosuke Shibasaki[1]
[1] JSPS Fellow, Lecturer, and Professor with the Center for Spatial Information Science, The University of Tokyo
5-1-5 Kashiwanoha Kashiwa Chiba, 277-8568, Japan; Tel:+81-4-7136-4307
E-mail: heromiya@csis.u-tokyo.ac.jp, shiba@csis.u-tokyo.ac.jp

[2] Master student with the Institute of Industrial Science, The University of Tokyo,
Cw-503 4-6-1 Komaba, Meguro-ku Tokyo, 153-8505, Japan; Tel: +81-3-5452-6412enter for Spatial
E-mail: itabashi@iis.u-tokyo.ac.jp

[3] Researcher of the GEO Grid Research Group with the National Institute of Advanced Industrial Science and Technology,
Tsukuba Central 2, Umezono 1-1-1, Tsukuba, Ibaraki 305-8568, Japan
E-Mail: iwao.koki@aist.go.jp

KEYWORDS: global urban area map, ASTER, automated image selection, automated urban area mapping, multi-source classification, Learning with Local and Global Consistency, logistic regression

ABSTRACT: We developed an automated method of image selection and urban area mapping for developing high-resolution global urban area maps. The method was successfully implemented and applied to 3372 cities of more than 0.1 million people of the world. As the result, the algorithm of image selection determined 11802 scenes of ASTER/VNIR satellite images and yielded good combinations for more than 60% of the cities. For the merged satellite images with the determined combinations, we applied the automated method of urban area mapping in high resolution. The method was consist of semi-supervised classifications by a machine learning method, called Learning with Local and Global Consistency (LLGC), and integrating the LLGC-derived maps and existing maps by logistic regression. As the result, we acquired urban area maps of 15-m resolution originated from ASTER/VNIR images, which is much finer than 500-m resolution of existing urban area maps. The method had still much space to be improved, especially in avoiding cloud contaminations. However, the method would contribute to complete high-resolution urban area maps of the world and realizing Global Earth Observation Systems of System (GEOSS).

1. INTRODUCTION

Urbanization has been a main concern for regional and global environmental change (Foley et al. 2005) and socio-economic problems (Angel et al. 2005). Various kinds of studies have used satellite-derived global urban area maps to evaluate critical aspects of urbanization for global environmental change, such as size, scale and form of cities and conversion of land cover. The studies using global urban area map had provided valuable information of urbanization especially for less documented regions. As the studies on urbanization progressed, however, 1-km spatial resolution of global urban area map have gotten obsolete for measuring spatial structure of urban area in fine scale (Angel et al. 2005) and for modeling land use conversion with socio-economical variables (Nelson & Robertson 2007).

Developing high-resolution urban area map would be key issue for promoting new insights on urban dynamics. Several studies had developed urban area map only for their cases using high-resolution satellite images (e.g. Landsat, Terra/ASTER, IKONOS and Quickbird) and shown valuable outcome; however mapping urban area using high-resolution satellite images involves considerable time and labor cost. It prevents comprehensive and comparative studies on urban dynamics on world's cities.

We regard that automation of the procedures was the key issue to develop high-resolution urban area maps of the cities of the world. In this paper, we present an automated method of selecting satellite images and urban area mapping on the satellite images. We also conducted a practical experiment on 3372 cities of the world using thousands of high-resolution satellite images.

2. METHODOLOGY AND MATERIALS

2.1. Automated Selecting and Merging ASTER/VNIR Satellite Images

For the global urban area mapping, we used the ASTER/VNIR satellite images archived in Global Earth Observation Grid (GEO Grid) of AIST in Japan (Yamamoto et al. 2006). ASTER/VNIR has 15-m spatial resolution which is much finer than those of existing global urban are maps. In addition, it has been operated to complete cloud-free coverage of the world since 1999 (Yamaguchi et al. 1998). By the 12-year operation, it is expected to be retrieved without cloud contamination for all the cities of the world. We used the surface reflectance image data of ASTER/VNIR with atmospheric correction of Rayleigh scattering.

The procedure for selecting satellite images for a city from millions of scenes of ASTER/VNIR is as following: defining inclusion extent, within which we constructed a mosaic of satellite images for a target crowd of cities (COC); sending a spatial query to identify scenes covering the inclusion extent; and assigning the orders to reduce cloud contamination. Here, we describe each step.

For the urban area mapping, we had to define the spatial extent to be mapped. Fortunately, many existing maps of broad scale have already spatially indexed the cities of the world with geographical coordinates. Among them, we adopted GRUMP Settlement Points (GSP; http://sedac.ciesin.columbia.edu/gpw/) as a primary index of the cities. The first reason of using it is that it had an almost complete coverage for the cities of more than 1000 population. Second, it had been manually associated to geographical coordinates of the cities. This direct human input is indispensable for accurate association of place names with geographic data because insufficient information from the source prevents automatic matching (Doerr & Papagelis 2007). Third, GSP includes the estimated population of each city, which can be used to order a priority of the urban area mapping.

In some intensively populated region, the coordinates of the cities are mutually so close to be within a satellite images. If the urban area mapping were performed for each indexed city, the satellite image covering the cities would have more than one time of extra processing. To avoid such extra processing, we assembled the coordinates of the cities close to each other into a COC. The distance was set to 30 km considering the 60-km swath widths of the ASTER/VNIR. The inclusion extents were constructed with the extent of 30-km buffer from the assembled point coordinates of the COC.

By overlaying the inclusion extents onto the spatial database of ASTER/VNIR archive, we identified the candidates of the scenes to be merged for each COC. From the candidate, we determined the combination and the order of the scenes by the following procedure.

1. Order the candidate scenes by percentage of cloud contamination in decrement.
2. Check the necessity of the first candidate scene for keeping complete coverage on the COC. If the COC was still covered without the candidate scene, the candidate scene was assigned unnecessary, and vice versa.
3. Check the necessity of all the candidate scenes. The scenes assigned to be necessary were the combination with the least contaminated with cloud.
4. Order the scenes assigned to be necessary by percentage of cloud contamination incrementally.

2.2. Automated Urban Area Mapping from ASTER/VNIR

On the merged satellite images, we performed an automated algorithm to identify urban area in 15-m resolution originated from ASTER/VNIR (Miyazaki et al. 2010). The algorithm was consists of two steps: extracting urban area from ASTER/VNIR by Learning with Local and Global Consistency (LLGC; Zhou et al. 2003), a machine learning method of semi-supervised classification, and integrating the LLGC-derived map with existing urban area maps and terrain data by logistic regression. For the logistic regression, we defined the 30 sets of population of the model considering distribution of the training data. Due to limitation of pages, we will not include the description in this paper. For further detail, please see Miyazaki et al. (2010) and upcoming papers.

3. RESULT AND DISCUSSION

3.1. Selecting ASTER/VNIR Images for COCs

For the experiment, we used the 3734 data points of the subset with more than 0.1 million from the GSP. By the 30-km rule, the 3734 data points were assembled into 2214 COCs. The combinations of the scenes for the COCs were determined by the procedure of checking necessity. To reject apparently unusable scenes, we set constrain on

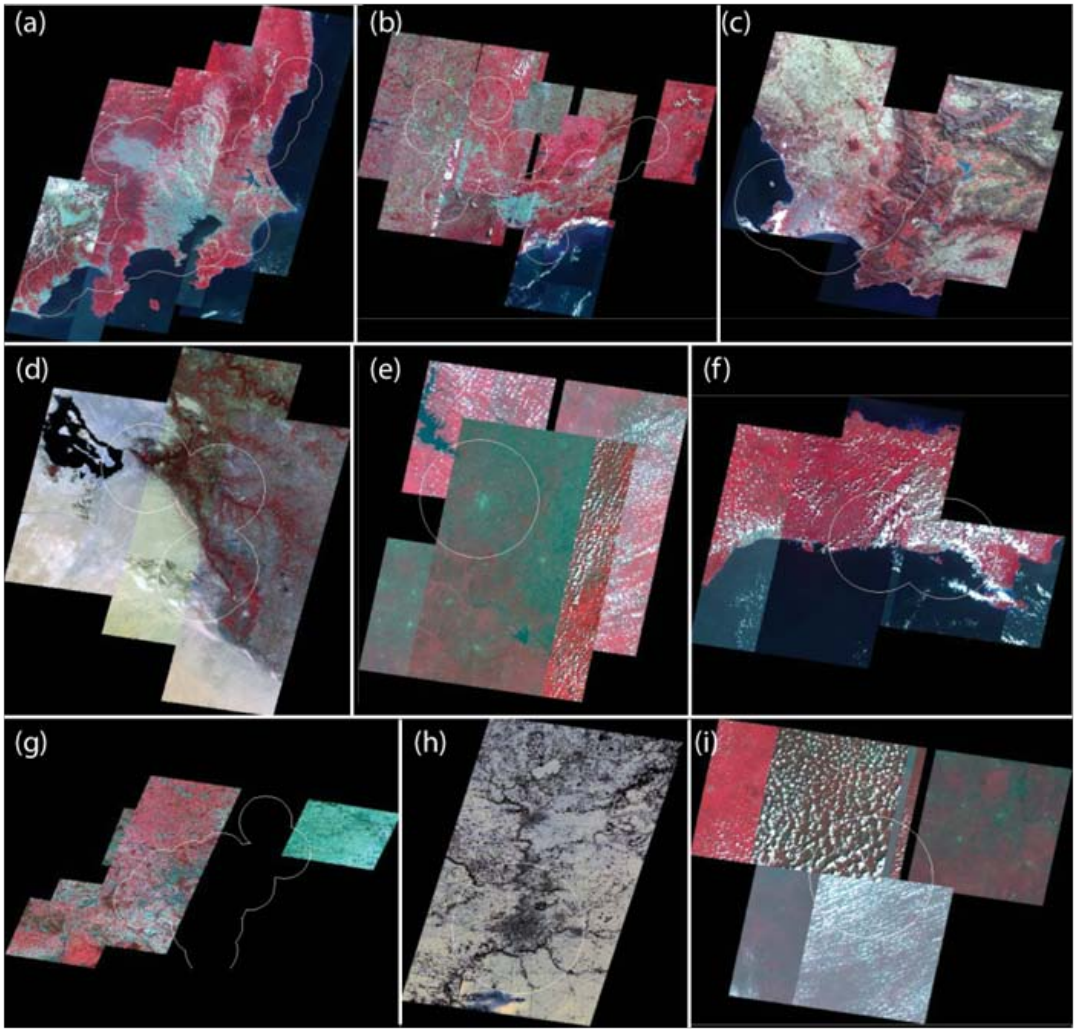

Figure 1. Examples of the results of automated selecting the ASTER/VNIR images. The background images are false color composite of the merged ASTER/VNIR. The white lines represents the boundary of the crowd of cities. (a) Tokyo (Japan), (b) Sao Paulo (Brazil), (c) Cape Town (South Africa), (d) Najaf (Iraq), (e) Yamoussoukro (Republic of Cote d'Ivoire), (f) La Romana (Dominican Republic), (g) Koln (Germany), (h) Rockford (United States of America), (i) Gagnoa (Republic of Cote d'Ivoire)

cloud contamination less than 20%. We also considered incidental failure of SWIR sensor, which is used for assessing cloud contamination, from 1 April in 2008, and set search period from the beginning to 31 March in 2008. As a result, for 1951 of the 2214 COCs, the combinations of the 11802 scenes were successfully assigned. For the other COCs, there was not any scene with condition of cloud contamination less than 20% over the search period. In this experiment, we rejected the 372 cities of the 263 COCs with incomplete coverage of ASTER/VNIR.

Figure 1 shows the examples of the results of merging the scenes with the combination assigned to be least-cloud contaminated. For 1340 of the 1951 COCs, the mosaic of ASTER/VNIR images were successfully organized; however, for the other 611 COCs, the combinations were incomplete to cover the extent of the COC or considerably contaminated with cloud. For the 611 COCs, we manually selected ASTER/VNIR images and ordered them (Figure 2). By the manual procedure, the visual appearances of the merged images were improved; however, some of them were still contaminated with cloud and haze.

In the selection of satellite images, cloud contamination was the main obstacle to determine the best combination of the satellite images. In this experiment, we used the database with rate of cloud contamination assessed by scene; therefore we could not reject cloud contamination partly occurred in the images. By assessing cloud contamination for each pixel (e.g. Tonooka et al. 2010), good-quality pixels of images partly contaminated with clouds would be combined with other good-quality pixels. Pixel-based assessment also would yield availability of the rejected images by less-than-20% criteria to be used for the urban area mapping, indicating that the pixel-based assessment

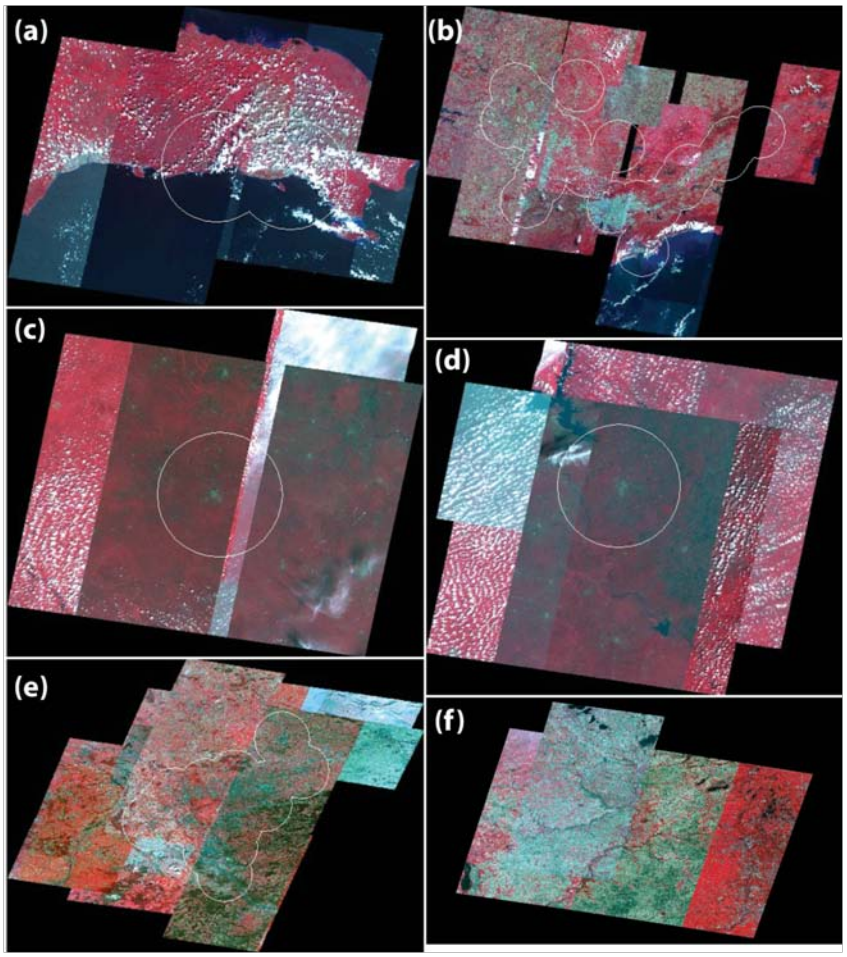

Figure 2. Examples of the results of manual selection of ASTER/VNIR images. The background images are false color composite of ASTER/VNIR. The white lines represent the boundary of the crowd of cities. (a) La Romana (Dominican Republic), (b) Sao Paulo (Brazil), (c) Gagnoa (Republic of Cote d'Ivoire), (d) Yamoussoukro (Republic of Cote d'Ivoire) , (e) Koln (Germany), (f) Rockford (United States of America)

would be necessary for completing the urban area map of the cities of the world.

3.2. Urban Area Mapping from the Merged images

We performed the automated algorithm of urban area mapping on the merged ASTER/VNIR images for the 1951 COCs. For the logistic regression, we prepared a set of training data including 10678 records of urban and 41610 records of non-urban. Figure 3 shows examples of the results. The urban area maps represented the spatial structure of urban area in much more detail than the urban area map derived from MODIS Terra + Aqua Land Cover Type Yearly L3 Global 500 m SIN Grid product for 2001 (Friedl et al. 2010; MCD12Q1), which was evaluated as the most accurate urban area map (Potere et al. 2009).

However, there were considerable misclassifications due to cloud contamination (e.g. the map for La Romana of Figure 3d). Such misclassifications were likely to be more in tropical zone, where there seemed to be much cloud contaminations of the ASTER/VNIR images, than those in other climatic zones. Also, there were misclassifications seemed to be associated to similarity of surface reflectance between urban and non-urban without vegetation (e.g. sand and vegetation). We found such misclassifications were likely to be appeared especially around desert cities (e.g. the map for Najaf of Figure 3c).

4. CONCLUSION

In this paper, we presented the method to develop the high-resolution global urban area map from ASTER/VNIR satellite images. The main issues were automation of two procedures: selecting satellite images and extracting urban area from the satellite images. Regarding the issue of selection, we proposed and implemented an automated

algorithm to select the best combination of satellite images covering a target COC. The experimental results showed that there were considerable spaces to be improved for complete coverage of urban area maps, especially with assessing cloud contaminations. We found that omitted cloud contaminations from the assessment were major causes of inferior quality of the urban area maps. We regard that introducing pixel-by-pixel assessment of cloud contamination is needed for better quality of the urban area maps.

The method had still much space to be improved; however, we regard that, with the improvement, it would be a great contribution to completing high-resolution urban maps of the world and realizing Global Earth Observation Systems of System (GEOSS).

ACKNOWLEDGMENT

This research used ASTER Data beta processed by the AIST GEO Grid from ASTER Data owned by the Ministry of Economy, Trade and Industry of Japan. The study was supported by a grant from Grant-in-Aid for JSPS Fellows (22-2598).

REFERENCES

Angel, S., Sheppard, S.C. & Civco, D.L., 2005. The Dynamics of Global Urban Expansion.

Doerr, M. & Papagelis, M., 2007. A Method for Estimating the Precision of Placename Matching. *IEEE Transactions on Knowledge and Data Engineering*, 19(8), pp.1089-1101.

Foley, J.A. et al., 2005. Global Consequences of Land Use. *Science*, 309(5734), pp.570-574.

Friedl, M.A. et al., 2010. MODIS Collection 5 global land cover: Algorithm refinements and characterization of new datasets. *Remote Sensing of Environment*, 114(1), pp.168-182.

Miyazaki, H. et al., 2010. Global Urban Area Mapping in High Resolution using ASTER Satellite Images. In *International Archives of the Photogrammetry, Remote Sensing and Spatial Information Science*. Kyoto, pp. 847-852.

Nelson, G.C. & Robertson, R.D., 2007. Comparing the GLC2000 and GeoCover LC land cover datasets for use in economic modelling of land use. *International Journal of Remote Sensing*, 28(19), pp.4243-4262.

Potere, D. et al., 2009. Mapping urban areas on a global scale: which of the eight maps now available is more accurate? *International Journal of Remote Sensing*, 30(24), pp.6531-6558.

Tonooka, H. et al., 2010. ASTER cloud coverage reassessment using MODIS cloud mask products. In X. Xiaoxiong, K. Choen, & S. Haruhisa, eds. SPIE, p. 78620S.

Yamaguchi, Y. et al., 1998. Overview of Advanced Spaceborne Thermal Emission and Reflection Radiometer (ASTER). *IEEE Transactions on Geoscience and Remote Sensing*, 36(4), pp.1062-1071.

Yamamoto, N. et al., 2006. GEO Grid: Grid Infrastructure for Integration of Huge Satellite Imagery and Geoscience Data Sets. In *Proceedings of The Sixth IEEE International Conference on Computer and Information Technology*. p. 75.

Zhou, D. et al., 2003. Learning with Local and Global Consistency. *Advances in Neural Information Processing Systems*, 16, pp.321-328.

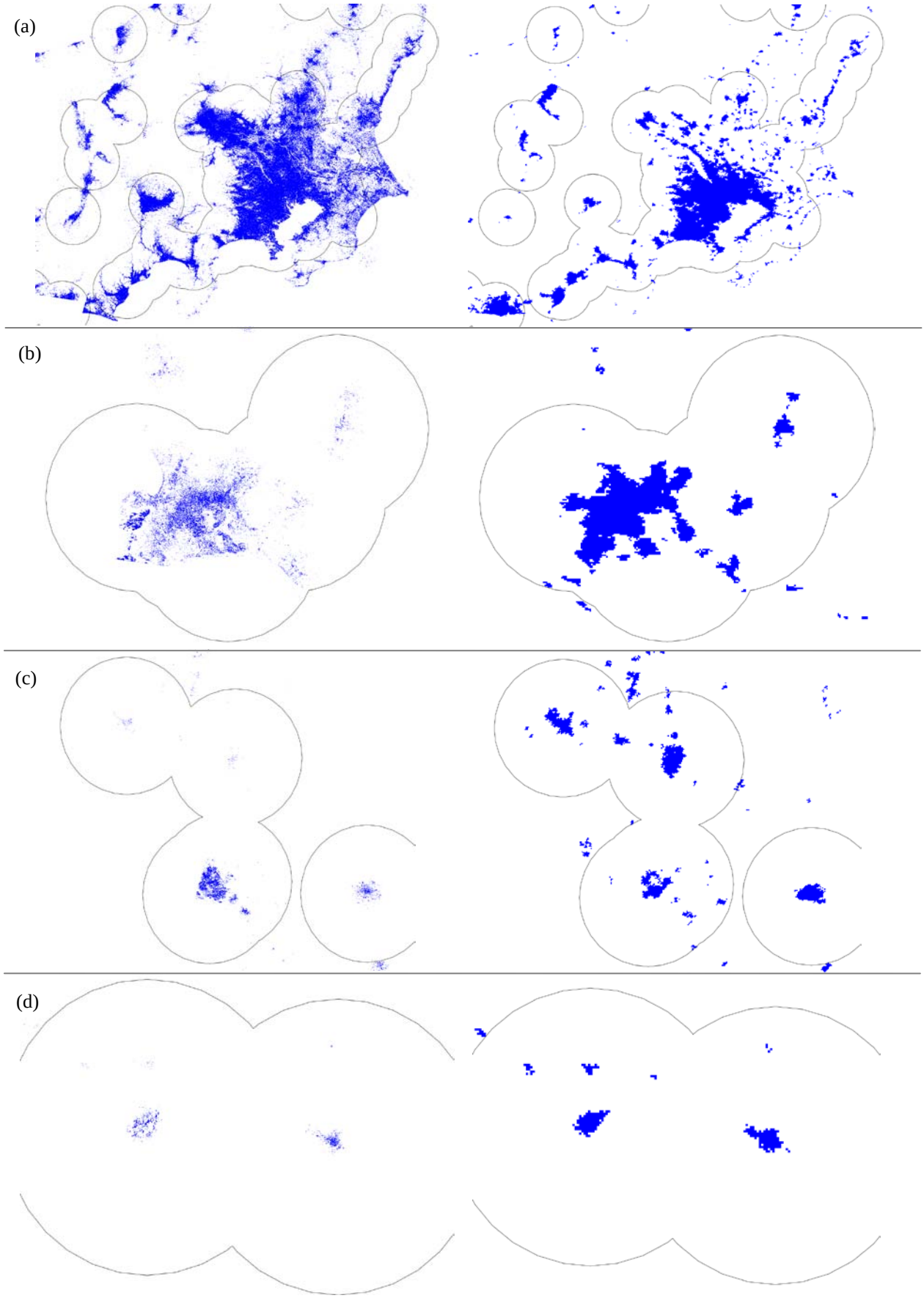

Figure 3. Examples of the results of urban area mapping. The left column represents the high-resolution urban area map. The right column represents urban and built-up class of MCD12Q1. The blue pixels represent to be assigned as urban. The lines represent the boundary of the COCs. (a) Tokyo (Japan), (b) Cape Town (South Africa), (c) Najaf (Iraq), (d) La Romana (Dominican Republic)